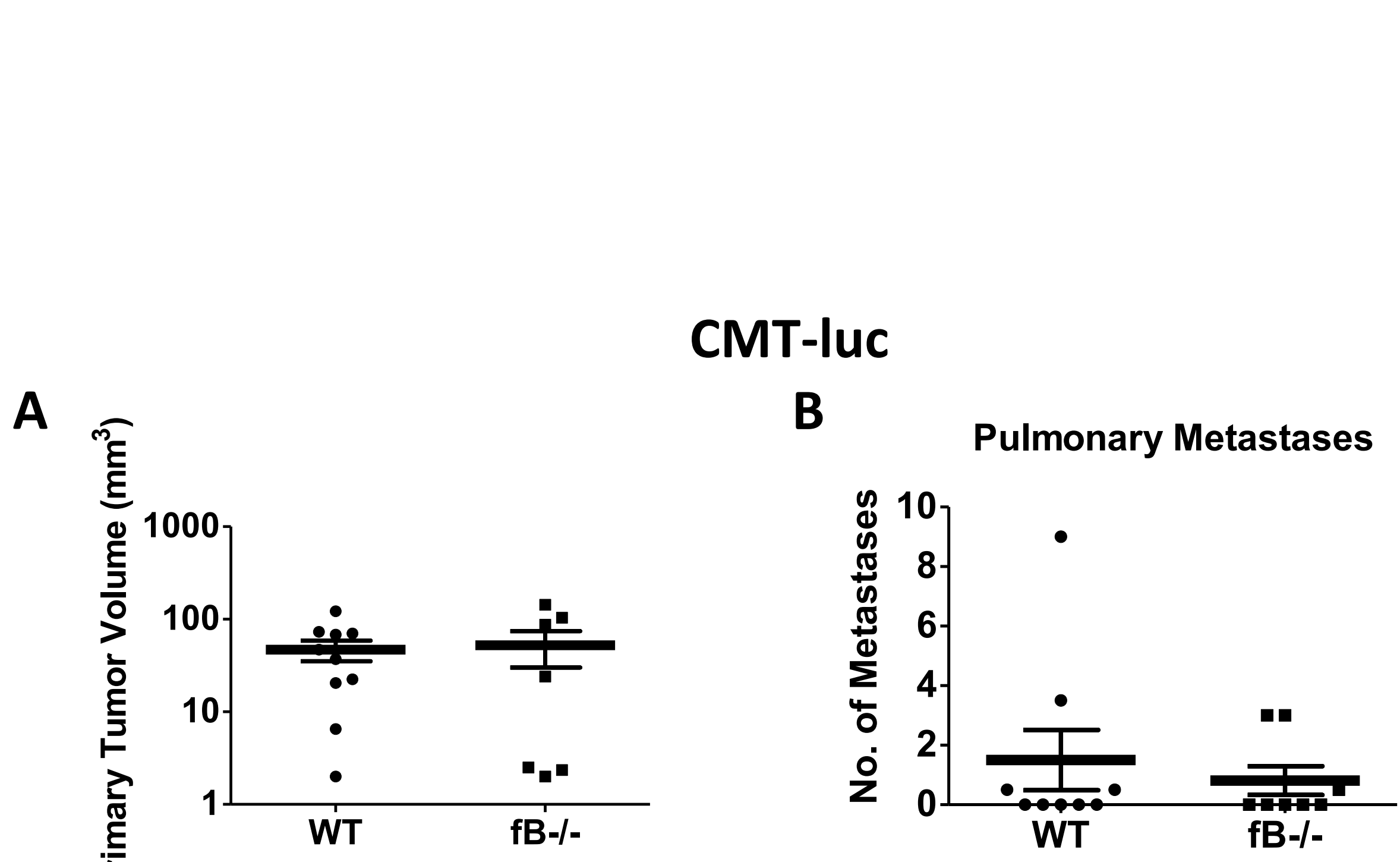

Supplemental Figure 1. Tumor Growth in factor B$^{-/-}$ mice (A and B) Primary tumor volumes and the number of metastases to secondary pulmonary spaces 28 days after CMT-luc implantation in WT or fB$^{-/-}$ mice are shown. Error bars represent mean ± SEM.

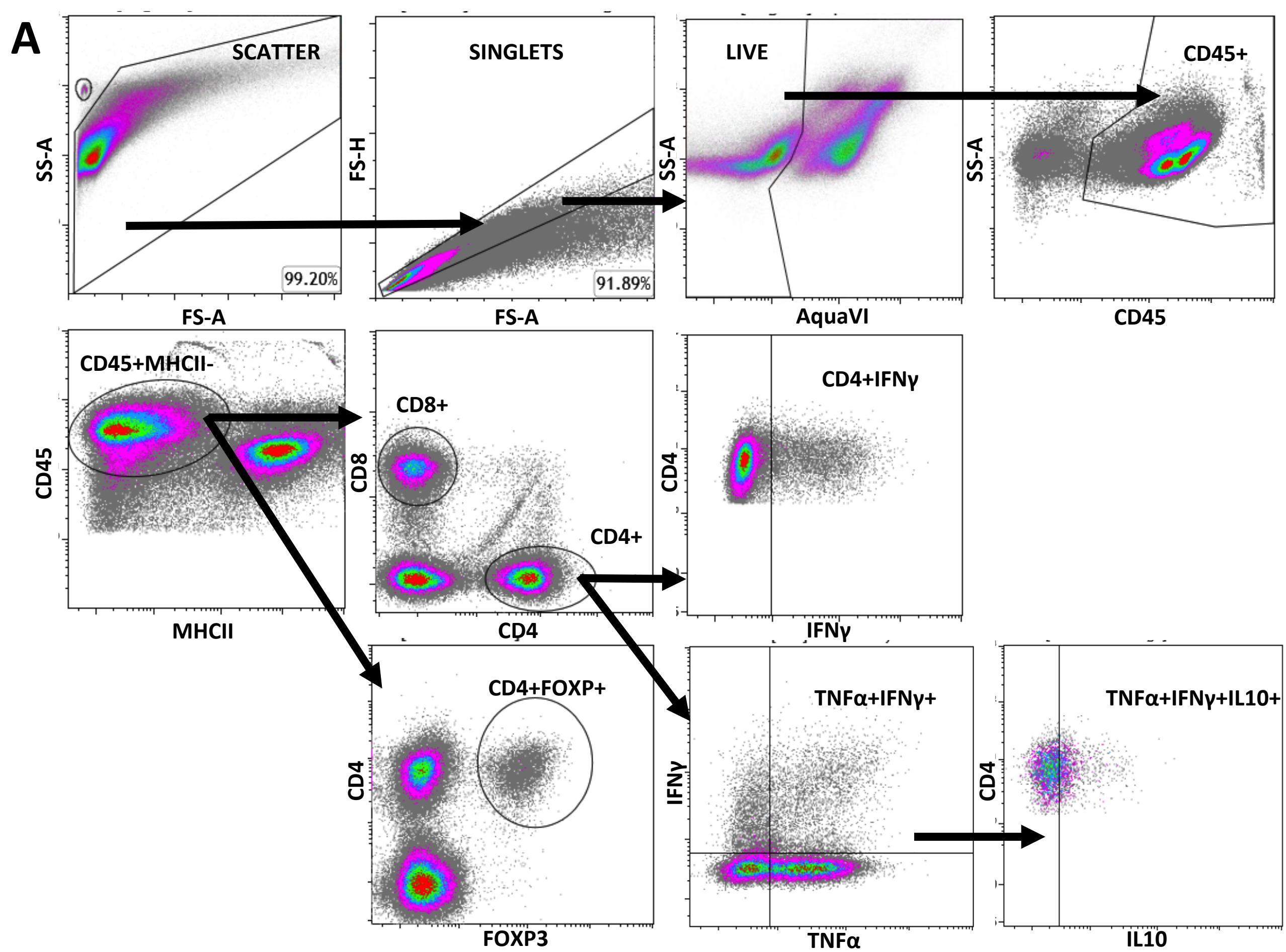

Supplemental Figure 2. Alterations in inflammatory and immune cells in CMT-luc tumor bearing mice. (A) Flow cytometric gating strategy to characterize CD4+ and CD8+ T cell populations of cytokine expression is shown. (B) Representative flow cytometric plots of isotype gating for indicated stain(s) are shown.

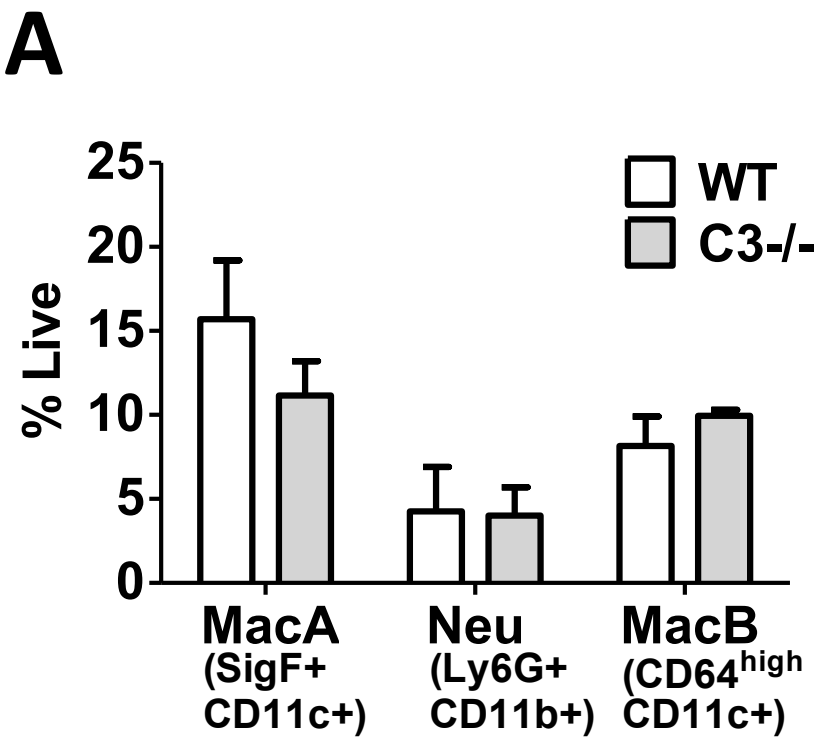

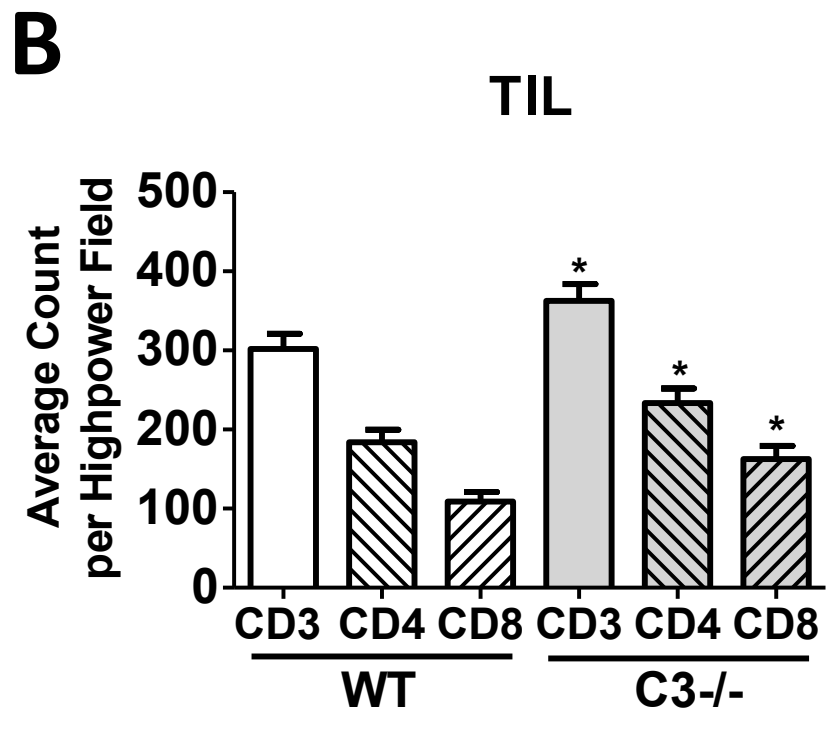

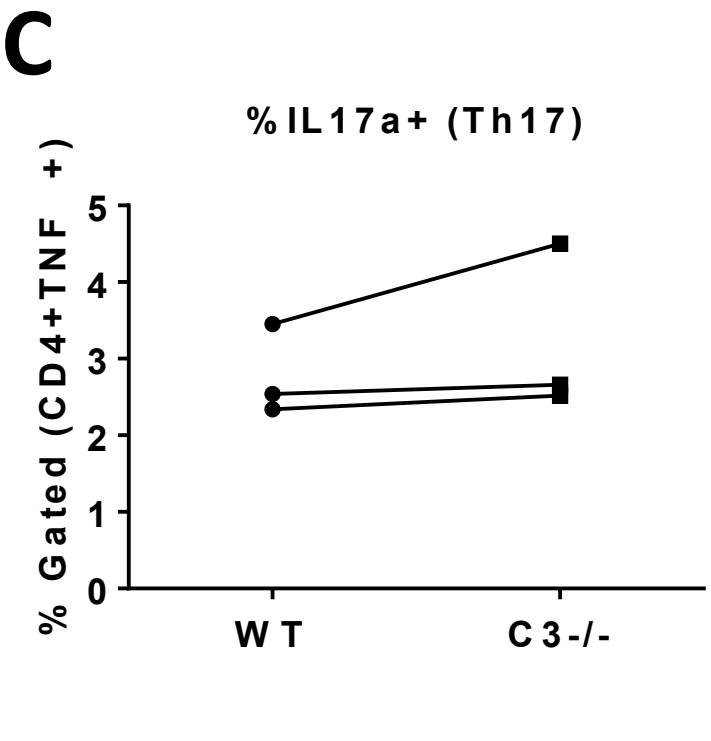

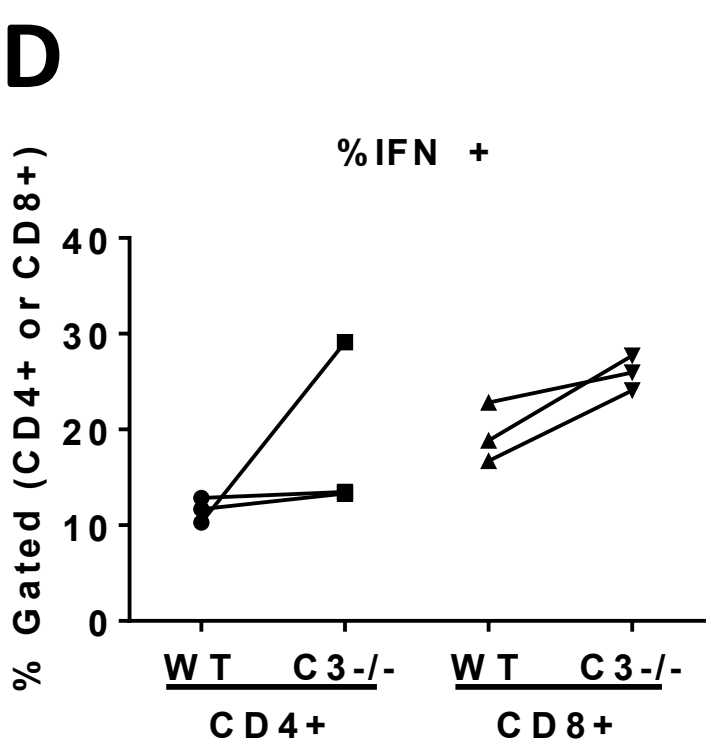

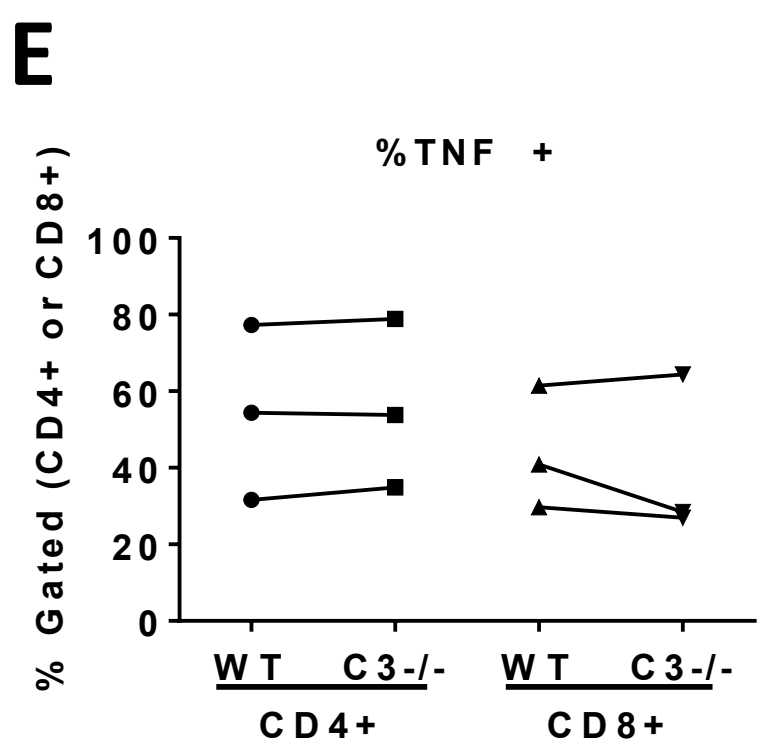

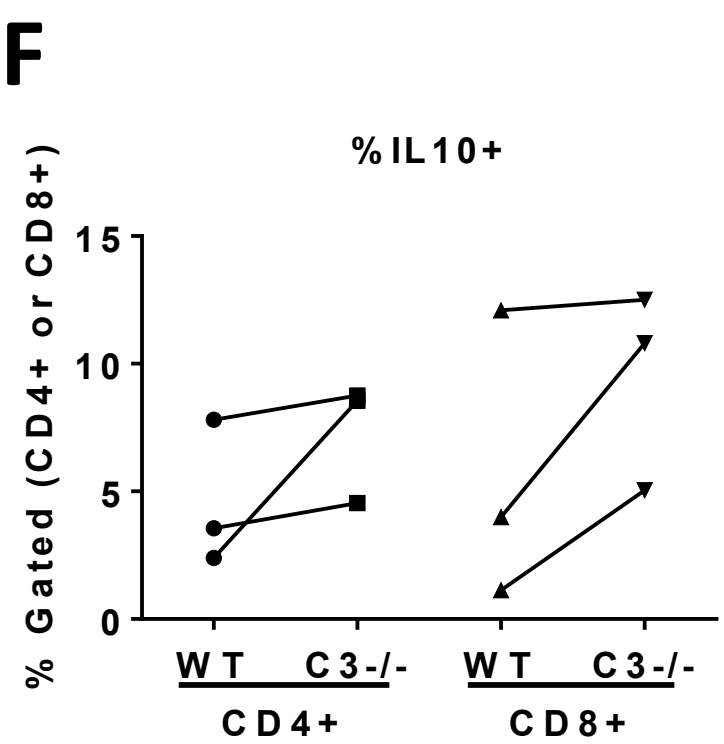

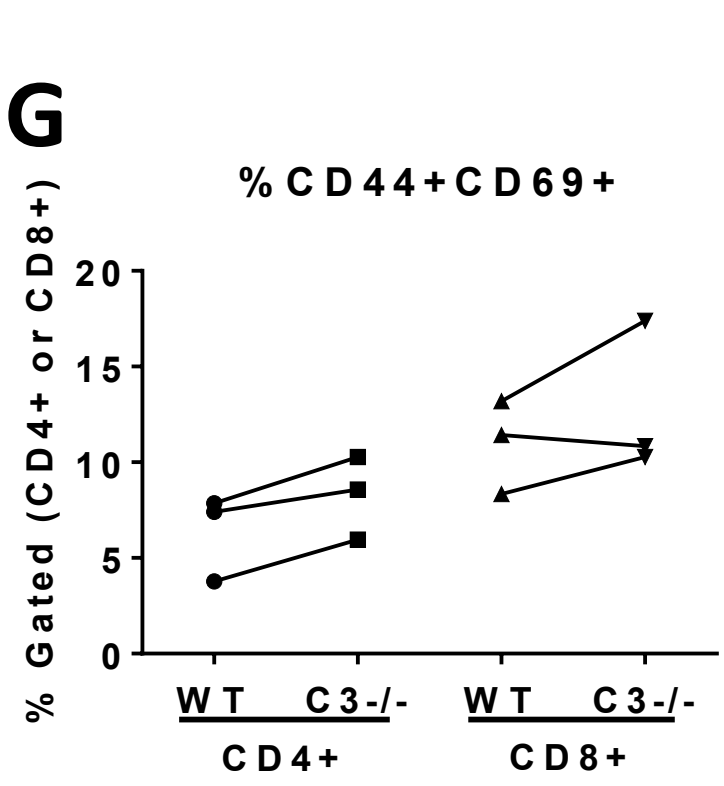

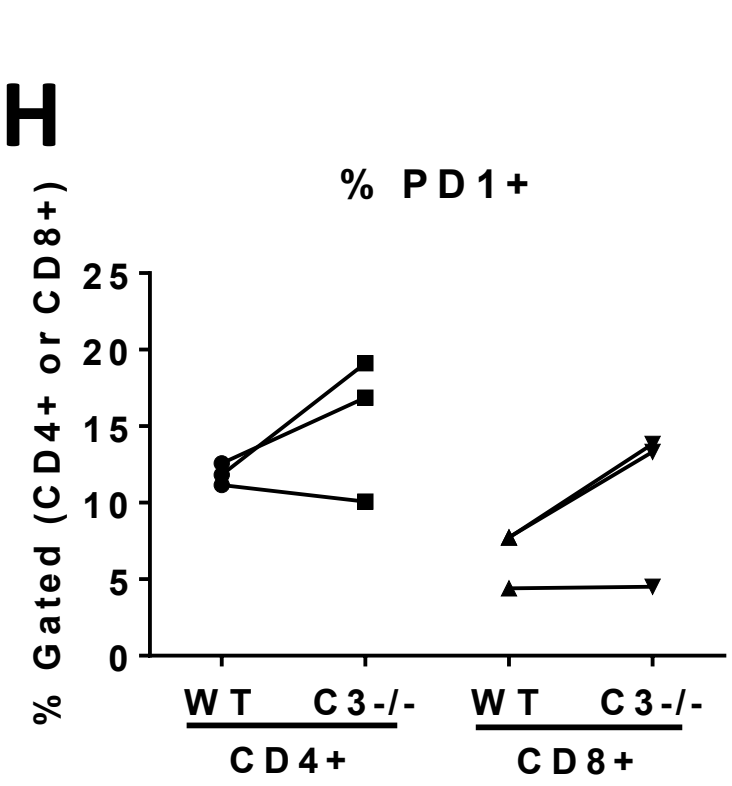

Supplemental Figure 3. Alterations in inflammatory and immune cells in CMT-luc tumor bearing mice. CMT-luc tumor-bearing lungs were analyzed by flow cytometry 7 and 10 days after implantation for the inflammatory populations and immune populations, respectively. (A) Average counts of tumor infiltrating CD3+, CD4+, or CD8+ cells per high power field (40x) within the day 10 CMT-luc primary tumors were assessed by immunofluorescence staining (WT n = 6; $C3^{-/-}$ n = 4). (B) Percentages of MacA (SigF+CD11c+), Neutrophils (Ly6G+CD11b+), and MacB ($CD64^{high}$CD11c+) of live cells 7 days after CMT-luc tumor implantation are shown (n = 2). The identification and flow strategy to identify the inflammatory populations are as previously described (26). (C-G) Each group represents 3 replicates of pools of 3 mice. (C) Percentages of IL-17a+ of CD4+TNFα+ T cells are shown. Percentages of (D) IFNγ+, (E) TNFα+, (F) IL10+, and (G) CD44+CD69+ (H) PD1+ of CD4+ or CD8+ cells are shown. Error bars represent mean ± SEM.

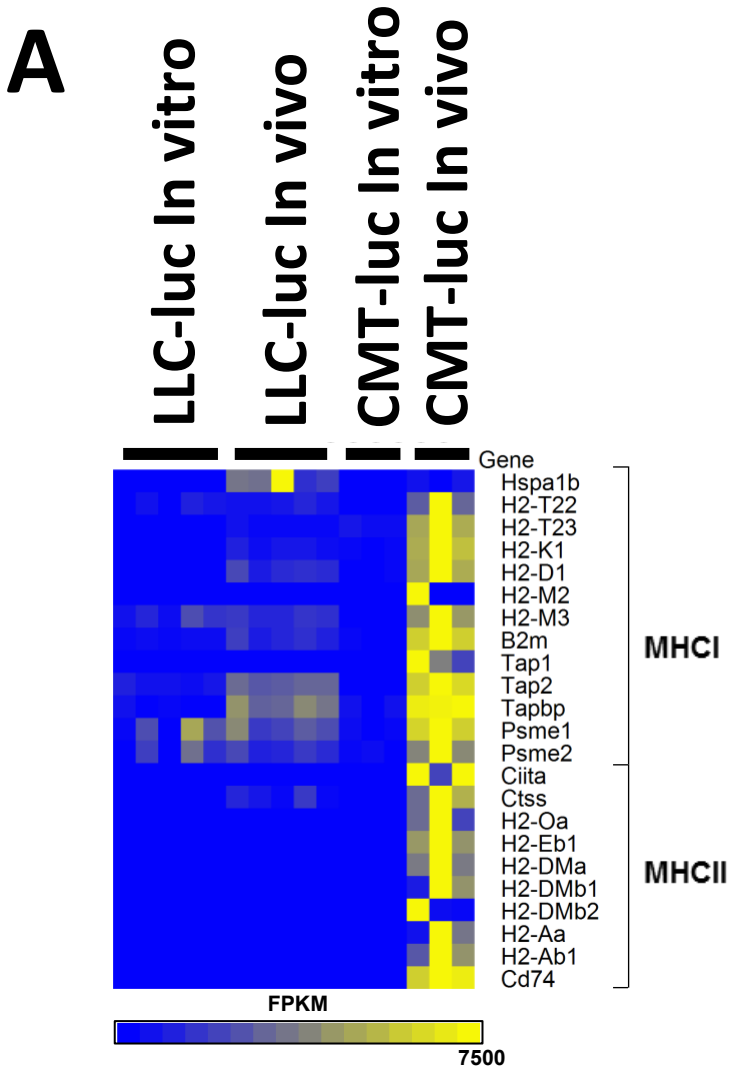

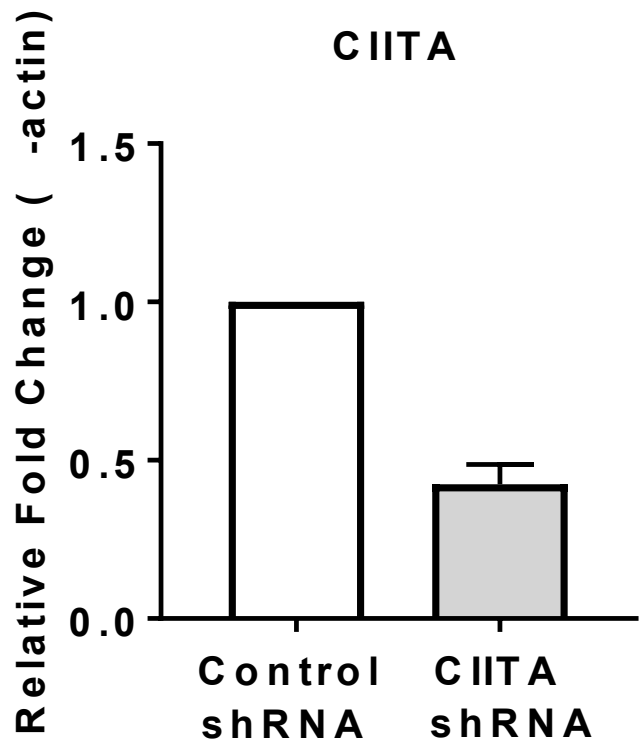

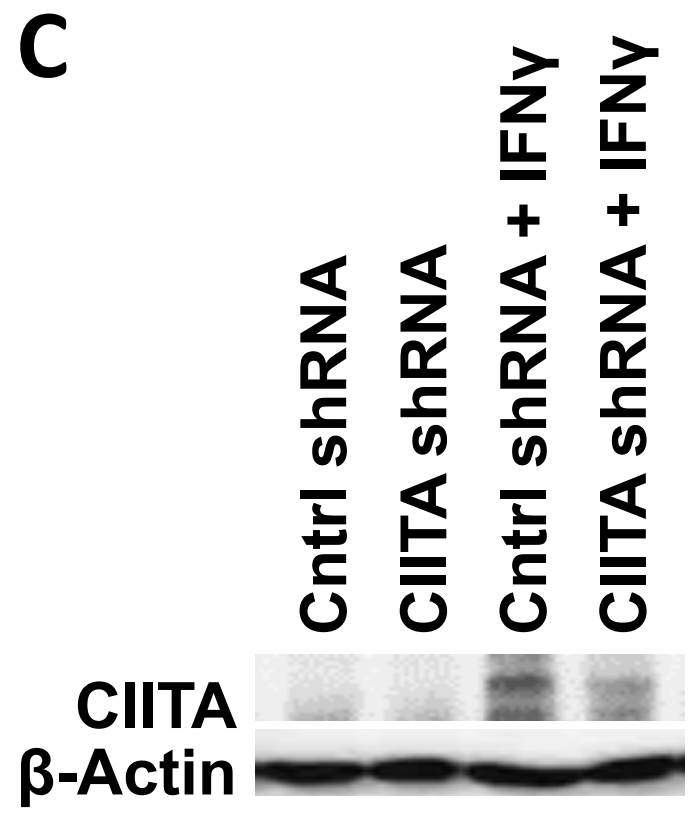

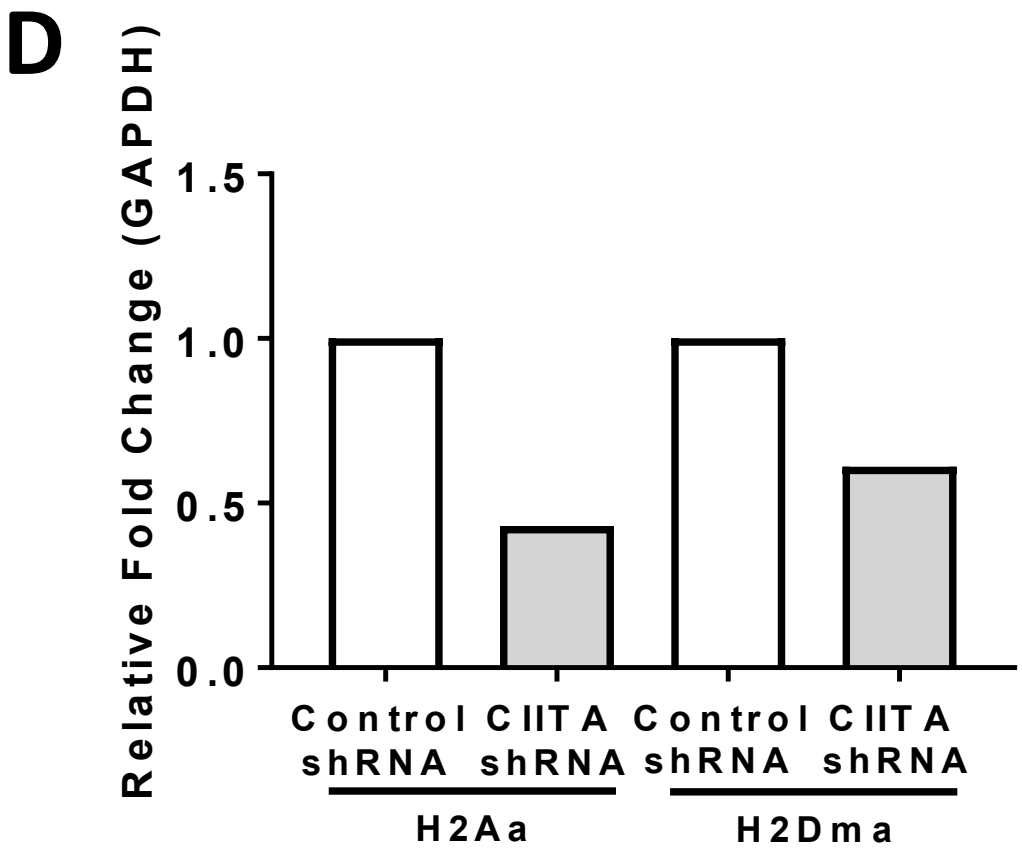

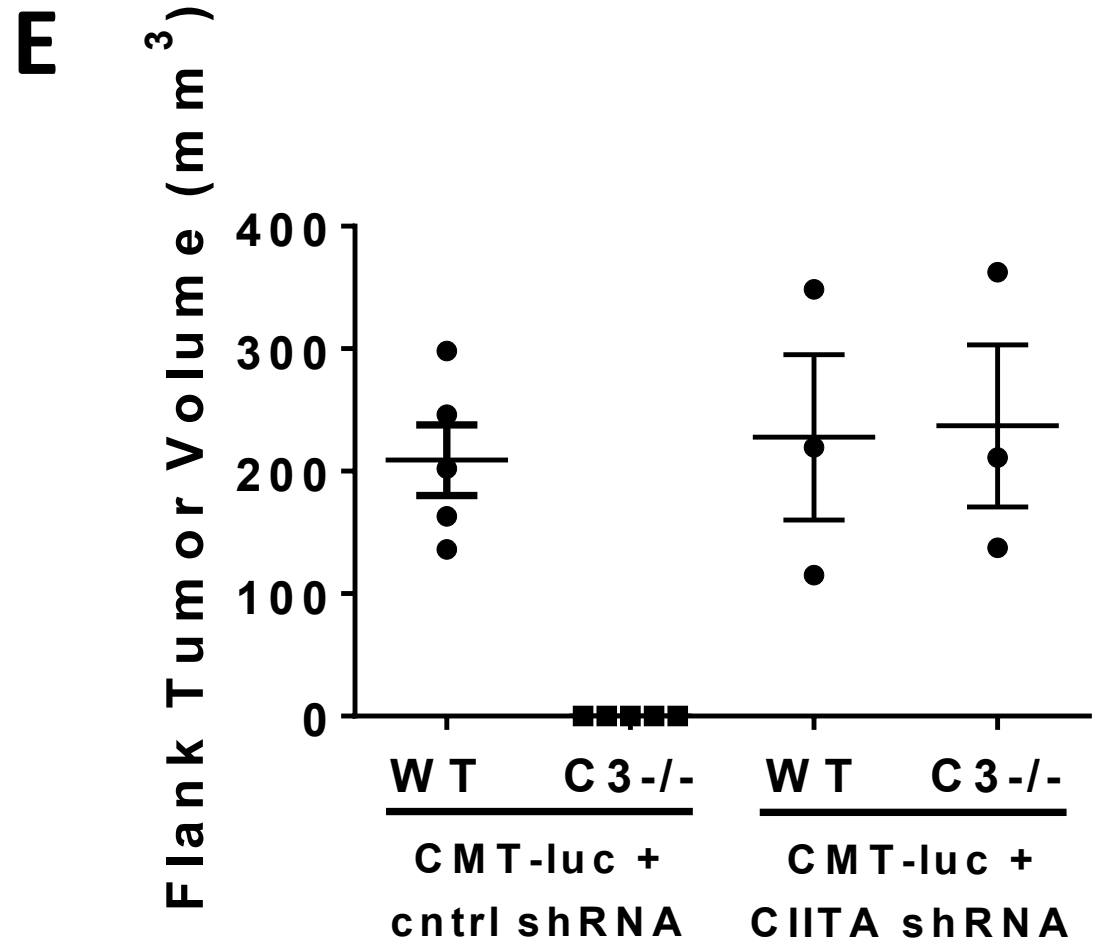

Supplemental Figure 4. Inhibition of CiiTA Expression in CMT-luc Confers the Gain of Growth in C3-/- Mice. (A) Heat map of the expression of MHC Class I and Class II genes in CMT-luc and LLC-luc cells in vitro versus in vivo is shown. (B-C) CiiTA gene and protein expression measured in CMT-luc with shRNA against CiiTA or scrambled control shRNA treated with IFNγ for 24hours by qPCR and WB are shown. (D) MHC Class II genes (H2Aa and H2Dma) expression of CMT-luc with CiiTA shRNA and control shRNA were measured by qPCR after 24hours of IFNγ treatment. (E) CMT-luc cells with CiiTA shRNA or control shRNA were injected into flanks of female WT or C3 deficient mice. The flank tumor volumes measured after 4 weeks are shown.

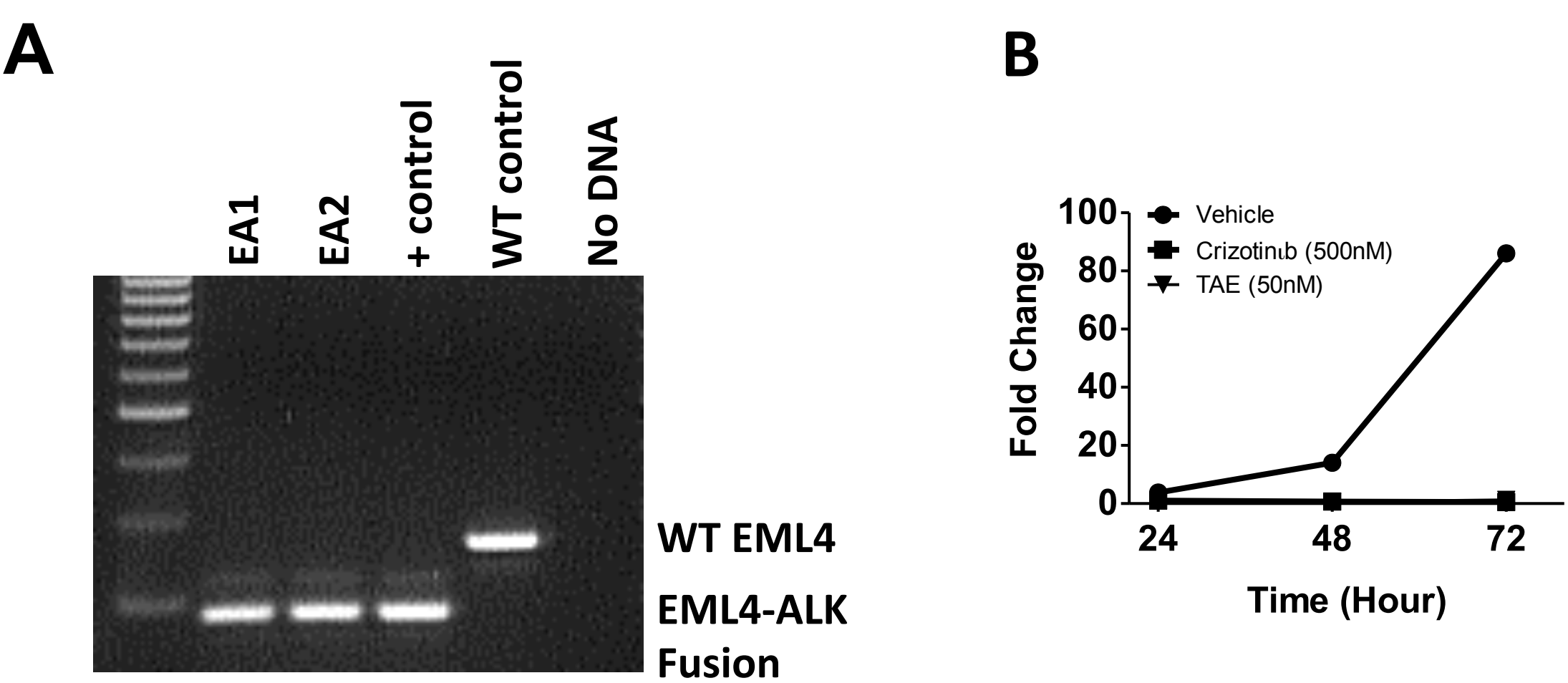

Supplemental Figure 5. Complement depletion inhibits tumor growth of EML4-ALK driven lung cancer cell line. (A) Genetic rearrangement of EML4-ALK in cultured tumor cells derived from animals treated with the Adenoviral construct as described previously (13). **(**B) Fold changes *in vitro* proliferation of EA2 cell line with treatment of Crizotinib (500nM) or TAE684 (50nM) are shown. (C) Primary tumor volumes 28 days after EML4-ALK implantation are shown, comparing WT and $C3^{-/-}$ recipients (n = 4). *p <0.05. Error bars represent mean ± SEM.

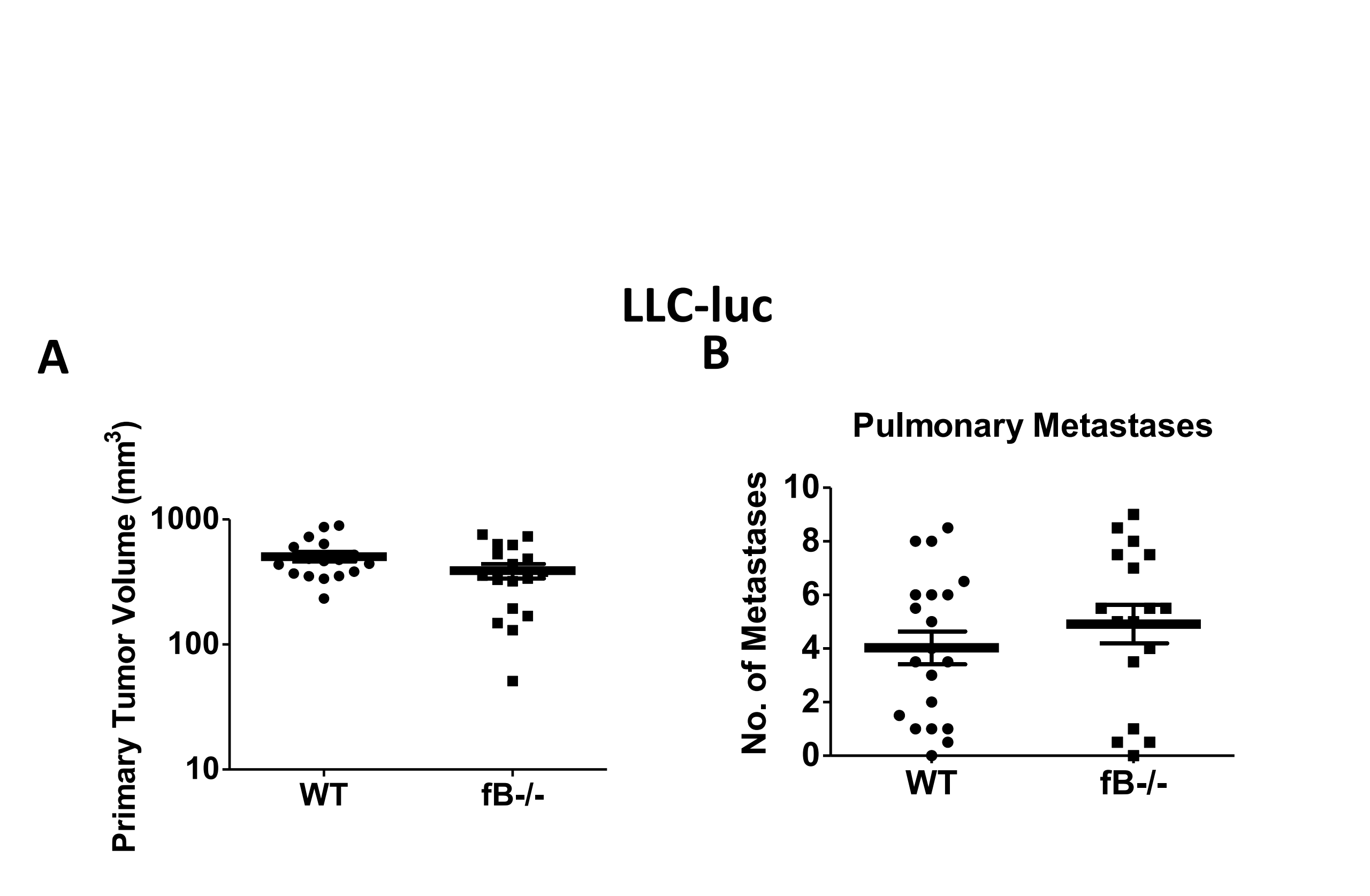

Supplemental Figure.6 LLC Tumor Growth in factor B$^{-/-}$ mice (A and B) Primary tumor volumes and the number of metastases to secondary pulmonary spaces 28 days after LLC-luc implantation in WT or fB$^{-/-}$ mice are shown. Error bars represent mean ± SEM.

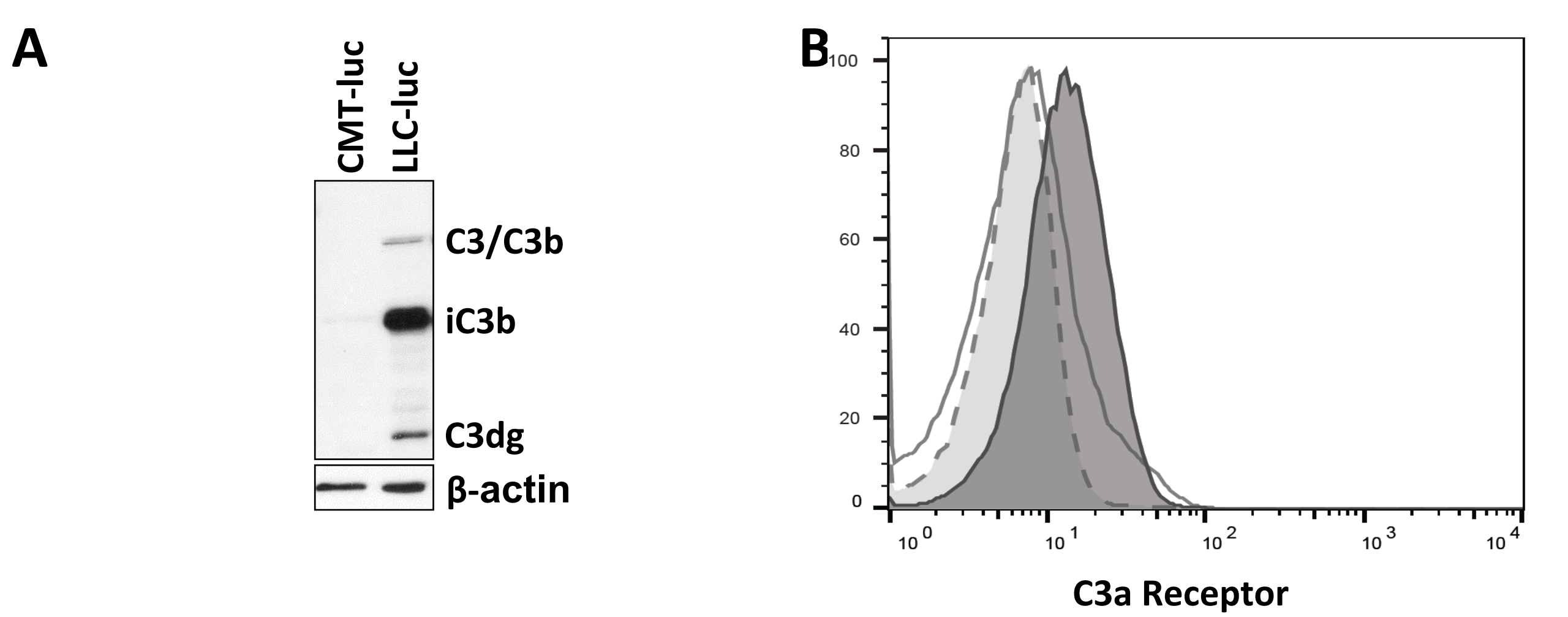

Supplemental Figure 7. LLC-luc lung cancer cell line expresses C3 and C3aR. (A) Western blot analysis of the whole cell lysates from CMT-luc and LLC-luc cells are shown. (B) Flow cytometric analysis of cell surface C3a receptor expression on CMT-luc and LLC-luc cell lines. (Isotype in dotted line (median = 7.35); CMT-luc in light grey (median = 10.2); LLC-luc in dark grey (median = 15.6))